UNIVERSITY OF LEEDS

This is a repository copy of *The role of inherited lithospheric heterogeneities in defining the crustal architecture of rifted margins and the magmatic budget during continental breakup*.

White Rose Research Online URL for this paper:
http://eprints.whiterose.ac.uk/144386/

Version: Published Version

Article:
Gouiza, M orcid.org/0000-0001-5438-2698 and Paton, DA orcid.org/0000-0001-8918-6697 (2019) The role of inherited lithospheric heterogeneities in defining the crustal architecture of rifted margins and the magmatic budget during continental breakup. Geochemistry, Geophysics, Geosystems, 20 (4). pp. 1836-1853.

https://doi.org/10.1029/2018GC007808

Reuse
Items deposited in White Rose Research Online are protected by copyright, with all rights reserved unless indicated otherwise. They may be downloaded and/or printed for private study, or other acts as permitted by national copyright laws. The publisher or other rights holders may allow further reproduction and re-use of the full text version. This is indicated by the licence information on the White Rose Research Online record for the item.

Takedown
If you consider content in White Rose Research Online to be in breach of UK law, please notify us by emailing eprints@whiterose.ac.uk including the URL of the record and the reason for the withdrawal request.

White Rose university consortium
Universities of Leeds, Sheffield & York

eprints@whiterose.ac.uk
https://eprints.whiterose.ac.uk/

Geochemistry, Geophysics, Geosystems

RESEARCH ARTICLE
10.1029/2018GC007808

Key Points:
- Labrador margin exhibits major along-strike changes of rift geometry, crustal architecture, and magmatic budget during continental breakup
- Pre-rift inheritance controls the initial lithosphere rheology, and lateral strength variations dictate the mode of rifting and breakup
- Magmatic budget during breakup is a function of mantle composition and timing and degree of hyperextension

Supporting Information:
- Supporting Information S1
- Figure S1

Correspondence to:
M. Gouiza,
m.gouiza@leeds.ac.uk

Citation:
Gouiza, M., & Paton, D. A. (2019). The role of inherited lithospheric heterogeneities in defining the crustal architecture of rifted margins and the magmatic budget during continental breakup. *Geochemistry, Geophysics, Geosystems*, *20*, 1836–1853. https://doi.org/10.1029/2018GC007808

Received 3 JUL 2018
Accepted 27 MAR 2019
Accepted article online 1 April 2019
Published online 12 APR 2019

©2019. American Geophysical Union. All Rights Reserved.

The Role of Inherited Lithospheric Heterogeneities in Defining the Crustal Architecture of Rifted Margins and the Magmatic Budget During Continental Breakup

Mohamed Gouiza[1] **and Douglas A. Paton**[1]

[1]Basin Research Group, Institute of Applied Geoscience, School of Earth and Environment, University of Leeds, Leeds, UK

Abstract During the final stage of continental rifting, stretching localizes in the future distal domain where lithospheric necking occurs resulting in continental breakup. In magma-poor margins, the lithospheric necking is accompanied by crustal hyperextension, serpentinization, and exhumation of mantle lithosphere in the continent-ocean transition domain. In magma-rich margins, the necking is accomplished by the emplacement of large amounts of volcanics in the continental-ocean transition, in the form of seaward dipping wedges of flood basalts (seaward dipping reflections). This study examines the factors controlling the final crustal architecture observed in rifted margins and the magmatic budget during continental breakup, using observations from the Labrador Sea. The latter shows magma-rich breakup with seaward dipping reflections documented in the north and magma-poor breakup with a wide domain of exhumed serpentinized mantle recorded in the south. The pre-rift strength of the lithosphere, defined by the inherited thermal structure, composition, and thickness of the lithospheric layers, controls the structural evolution during rifting. While variations in the magmatic budget associated with breakup are controlled primarily by the interaction between the pre-rift inheritance, the timing and the degree of mantle melting, in relation to lithospheric thinning and mantle hydration.

1. Introduction

Despite the observed variations in the structural style, sedimentary architecture, and magmatic budget of rifted margins, they usually show a strikingly similar crustal-scale anatomy characterized by continental and oceanic domains, separated by a transitional domain (Manatschal, 2004; Mohn et al., 2012). The continental domain is where crustal extension takes place and it is characterized by a weakly deformed/thinned proximal crust, a necking zone with a shallowing of the Moho, and a highly thinned distal crust. The transition from continental to oceanic crust occurs over a transitional domain where breakup processes localize before the initiation of continental drifting and accretion of oceanic crust (Lavecchia et al., 2017; Soares et al., 2012).

The continent-ocean transition (COT) is best studied and understood in magma-poor (i.e., nonvolcanic) margins. This is particularly true with respect to the present-day Iberia-Newfoundland margins, where there is an abundance of high-resolution seismic data and deep ocean drillings (e.g., Manatschal, 2004; Péron-Pinvidic & Manatschal, 2009; Sutra & Manatschal, 2012), and in the Alps, where the ancient Mesozoic Tethys margins are preserved and exposed providing excellent field analogs (e.g., Epin & Manatschal, 2018). Observations indicate that the COT forms during the final stage of rifting when deformation in the crust and subcontinental mantle becomes coupled. The crustal faults are then rotated to low angle and form detachments that exhume the mantle prior to continental breakup (e.g., Manatschal, 2004).

In magma-rich (i.e., volcanic) rifted margins the nature of the crust in the COT and the nature of the geological processes involved in its formation are still debated. Two conceptual end-member models are proposed, which indicate that the COT consists of either a highly thinned continental crust heavily intruded by mafic dikes (Franke, 2013) or a newly formed magmatic crust emplaced before the formation of the true oceanic crust (Paton et al., 2017). Many magma-rich margins show the COT crust overlain by extrusive volcanics interbedded with sediments (i.e., SDR packages; Planke & Eldholm, 1994).

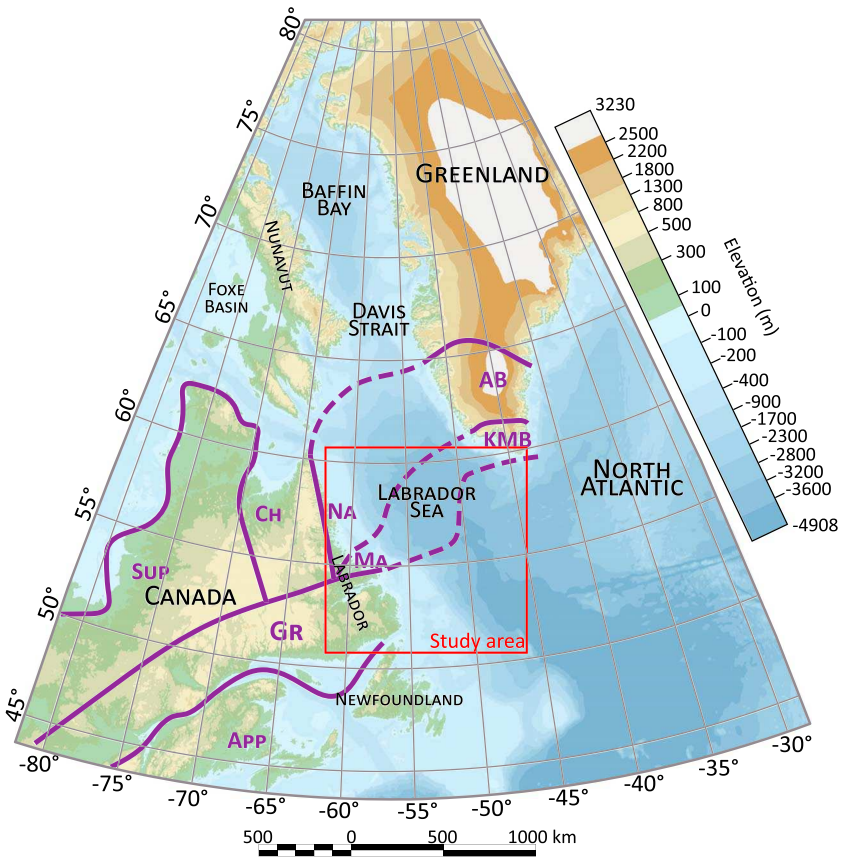

Figure 1. Regional map of east Canada and west Greenland showing the offshore North Atlantic basins (i.e., Labrador Sea, Davis Strait, and Baffin Bay) and the onshore pre-Mesozoic domains: Sup: Superior Province; Ch: Churchill Province; Na: Nain Province; AB: Archean Block; Ma: Makkovik Province; KMB: Ketilidian Mobile Belt; Gr: Grenville Province; App: Appalachian Province.

The distinction between magma-poor and magma-rich rifted margins is based mainly on the timing and degree of mantle melting in relation to lithosphere extension and continental breakup (Geoffroy et al., 2015). For instance, in the mid-Norway rifted margin, the Eocene magma-rich continental breakup was preceded by a Jurassic–Cretaceous phase of extreme crustal thinning in a magma-poor setting (i.e., hyperextension) (Osmundsen & Ebbing, 2008). The COT, where breakup volcanics are found, is bounded to the east by a 100- to 200-km wide continental domain of highly extended crust (i.e., 2- to 12-km thick). Low-angle detachments, similar to the ones observed in the Iberia margin, are believed to control the coupled stretching of the crust and the subcontinental mantle, which may have become exhumed if extension had continued (Osmundsen et al., 2016; Osmundsen & Ebbing, 2008; Péron-Pinvidic et al., 2016).

In this study, we use seismic reflection and potential field data from the west Labrador Sea margin (Figure 1) to constrain the style of extension during rifting and the subsequent different crust types. We also characterize the variation in magmatic supply associated with continental breakup along the margin by investigating the nature of the rocks in the COT domain using seismic data and gravity modeling. We show that the COT in the southern part of the Labrador margin is made of exhumed serpentinized mantle, while in the northern part it consists mainly of volcanics. We then investigate how inherited lateral changes in the thermal structure, composition, and thickness of the pre-rift lithospheric layers influence the structural evolution of rifted margins during rifting. We finally argue that inherited Precambrian structures and lithospheric heterogeneities controlled the structural evolution during rifting and the magmatic budget during breakup.

2. Geological Setting

The Labrador Sea is an oceanic basin that formed by seafloor spreading as a branch of the North Atlantic Ocean between Canada and west Greenland. Rifting in the North Atlantic began during the Late Triassic–Early Jurassic between Newfoundland and Iberia (e.g., Alves et al., 2009; Tucholke et al., 2007), and then by the Early Cretaceous rifting migrated northward between SW Greenland and Labrador (e.g., Dickie et al., 2011). The pre-Mesozoic basement of the Labrador Sea is well-exposed onshore Canada (Figure 1) and consists of three tectonic units, namely from north to south, the Archean Nain Province, the Paleoproterozoic Makkovik Province, and the Late Paleoproterozoic Grenville Province (Figure 1, Wardle et al., 1997). The Nain Province belongs to the North Atlantic Craton, which comprises several gneiss terranes that were imbricated during Archean tectonic events (e.g., Nutman et al., 2004). The Makkovik Province consists of reworked cratonic Archean rocks, juvenile units, and granitic intrusions, all of which were deformed during the ca. 1.90–1.78 Ga orogeny resulting from the assembly of Laurentia (Van Kranendonk et al., 1993). The Makkovik Province is separated from the Nain Province by the NE-SW trending Kanairiktok shear (Culshaw et al., 2000). The Grenville Province has a complex geological history with several tectonic phases (i.e., extensional and compressional) during the Paleoproterozoic and Mesoproterozoic (Gower, 1996). Its final structural configuration was achieved during the Grenvillian orogeny (1.08–0.97 Ga), which resulted in northwesterly thrusting and widespread plutonism (Gower, 1996). It is separated from the northern provinces by the Grenville Front, marking the northern limit of the Grenvillian deformation. Prior to the opening of the Labrador Sea, the Nain and Makkovik domains were, respectively, attached to the Archean Block and the Ketilidian Mobile Belt found in south Greenland (Figure 1, Wittig et al., 2010).

Extension in the Labrador Sea was accommodated mainly by NW-SE trending normal faults, which bounded grabens and half-grabens where syn-rift sediments were deposited (e.g., Balkwill & McMillan, 1990). The timing of the transition from continental rifting to oceanic accretion is much debated. The oldest proposed breakup age is ca. 92 Ma (Turonian), based on a major stratigraphic unconformity (Balkwill & McMillan, 1990), while the youngest proposed age is Paleocene (ca. 62 Ma), corresponding to the magnetic anomaly of Chron 27 (Chalmers & Laursen, 1995). In contrast, Chian et al. (1995) used wide-angle seismic to determine the crustal structure across the Labrador margin and their velocity model shows that the oceanic crust starts at Chron 31, which suggests an initiation of continental drifting during the Maastrichtian (ca. 68 Ma). Although magnetic anomalies in the Labrador Sea (Figure 2) are relatively well identified, the origin of the weak anomalies landward of Chron 27 remains largely disputed (e.g., Srivastava & Roest, 1999). Unlike anomalies 26–21 that are consistently interpreted to be oceanic, low-amplitude anomalies 34–27 were proposed to be related to dykes intruding stretched continental crust (Chalmers & Laursen, 1995), ultraslow seafloor spreading (Srivastava & Roest, 1999), or serpentinized mantle underlying very thin continental crust (Chian, Keen, et al., 1995).

The Labrador Sea is surrounded by the Newfoundland-Iberia margins in the south and by the Davis Strait and Baffin Bay margins in the north. The former experienced magma-poor breakup with a wide transitional domain made of exhumed subcontinental mantle (Péron-Pinvidic & Manatschal, 2009; Tucholke et al., 2007), while the latter is recognized as magma rich with seaward dipping reflections (SDRs) documented in the COT (Funck et al., 2007; Suckro et al., 2012). The rifted margins of the Labrador Sea are classified as magma poor in the south (Chian et al., 1995) and as magma rich in the north (Keen et al., 2012). Syn-rift to breakup magmatism is found onshore and offshore southwest Greenland and Labrador (Larsen et al., 2009; Peace et al., 2016 ; Tappe et al., 2007). Its distribution is, however, highly asymmetric with only minor Mesozoic magmatic intrusions exposed in the Labrador side, mainly in the Makkovik domain, compared to the widespread Jurassic to Cretaceous igneous rocks outcropping along the SW Greenland side (Peace et al., 2016; Tappe et al., 2007). Offshore rift-related magmatism is observed in wells on the Labrador shelf (no wells were drilled on the conjugate SW Greenland shelf), where basalt sequences are associated with the Lower Cretaceous Alexis formation deposited during the early phase of rifting (Umpleby, 1979). Extensive flood basalts, dated to be Early Paleocene and Early Eocene, are found around the Davis Strait (Funck et al., 2007; Larsen et al., 2009). Whereas the Paleocene volcanics are attributed to the passage of the proto-Icelandic plume north of the Labrador Sea, the Early Eocene volcanics could be related to a major change in plate motions in the North Atlantic region due to the Iceland plume (Dickie et al., 2011; Storey et al., 2007).

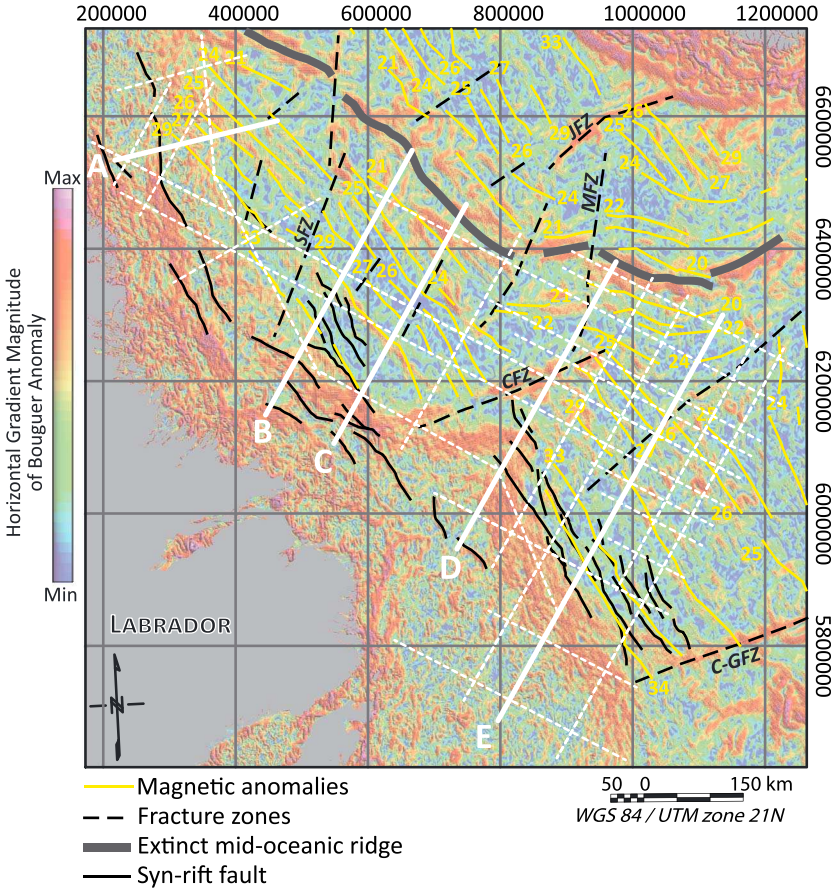

Figure 2. Map of the Labrador margin showing the location of the seismic lines used in this study (in white; courtesy of TGS), the offshore horizontal gradient magnitude (HGM) of the Bouguer anomaly, and the magnetic anomalies (according to Srivastava & Roest, 1999). Solid black lines are the syn-rift faults interpreted along the seismic lines (see Figure 3) and interpolated along the HGM highs. SFZ: Snorri Fracture Zone; CFZ: Cartwright Fracture Zone; MFZ: Minna Fracture Zone; JFZ: Julinhaab Fracture Zone; C-GFZ: Charlie-Gibbs Fracture Zone.

3. Data and Methods

This study relies on 31 regional seismic reflection lines acquired by TGS offshore the Labrador-Newfoundland margin (Figure 2). Since the main focus is on the syn-rift period leading to continental breakup in the Labrador Sea, two seismo-stratigraphic horizons were picked along the seismic lines, in addition to the seabed, namely, the top syn-tectonic unit and the top basement (Figure 3). The syn-tectonic unit is the seismo-stratigraphic package that is affected by the Cretaceous extension. Its top was defined as the horizon that drapes the extensional structures and that is probably of Maastrichtian to early Paleocene age.

Because the Moho is only partially imaged in the seismic data, mainly underneath the oceanic crust, we used satellite free-air gravity data (Sandwell et al., 2014) to constrain crustal thicknesses in the continental and oceanic domains. First, the interpreted seismic lines were depth converted using interval velocities defined in the nearby Orphan Basin (Gouiza et al., 2017). Then, GEOSOFT GM-SYS Profile Modelling was used to model the crustal architecture along the seismic lines (Pouliquen et al., 2017). The forward modeling was constrained by the seismic interpretation, except for the Moho depth (where poorly constrained by seismic) and densities in the COT, which were modified to achieve a reasonable fit between the observed and the calculated gravity. The gravity modeling was carried out assuming constant densities for the two sedimentary packages (2.45 and 2.30 g/cm^3 for the syn-tectonic and post-tectonic units, respectively), the upper continental crust (2.8 g/cm^3), lower continental crust (2.90 g/cm^3), oceanic crust (2.90 g/cm^3), and mantle (3.33 g/cm^3). These values fall within the range of densities derived from seismic velocities and gravity inversion in the Labrador margin (Funck et al., 2001, 2008; Welford & Hall, 2013). Funck et al.

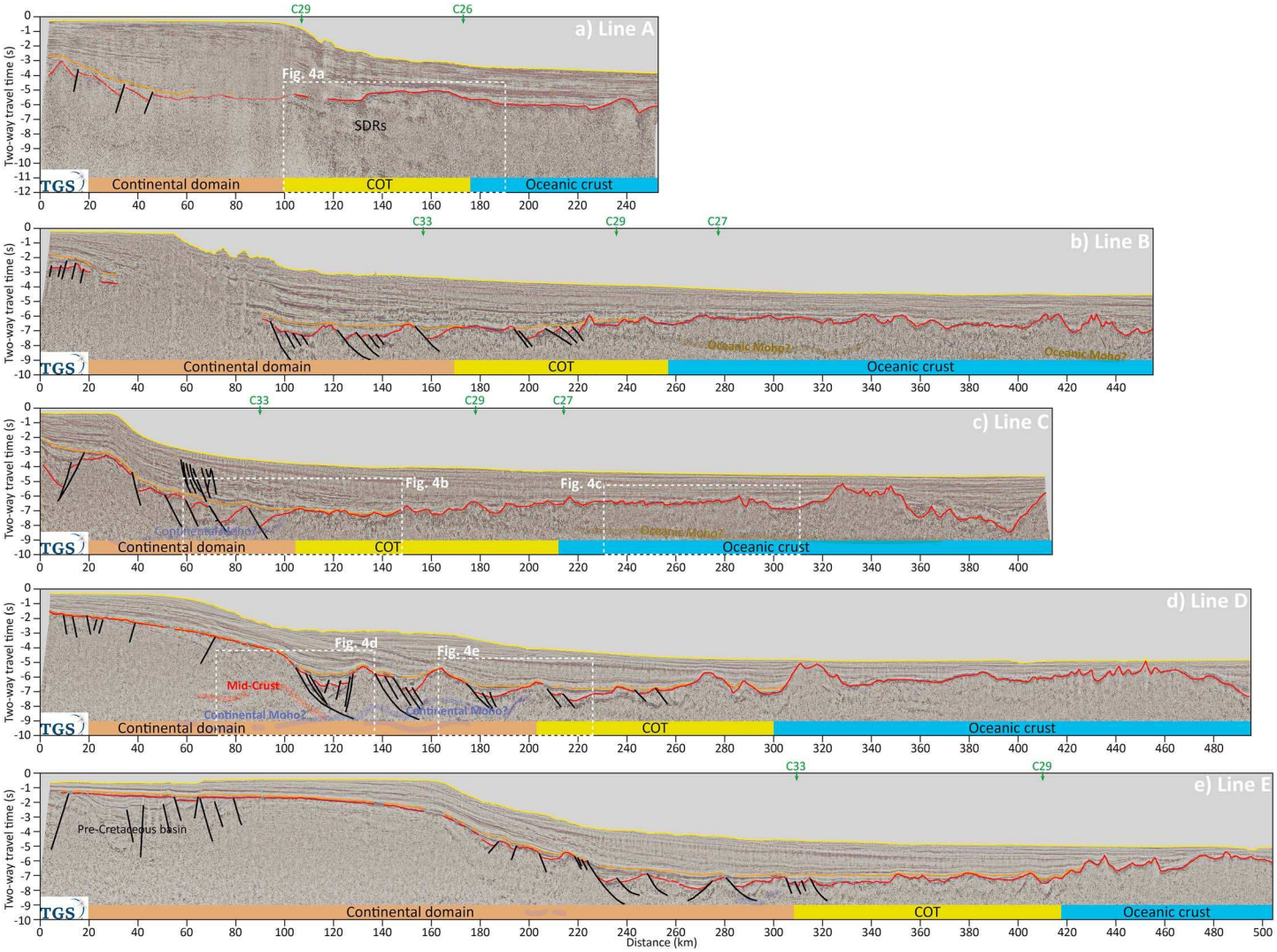

Figure 3. Interpreted seismic lines showing the tectono-stratigraphic architecture of the Labrador margin and the different crustal domains (i.e., continental, transitional, and oceanic). Red line: top pre-Cretaceous basement; orange line: top syn-tectonic sedimentary package; yellow line: seabed/top post-tectonic sedimentary package; black lines: interpreted faults. Green arrows indicate the location of the main magnetic Chrons (C).

(2001, 2008) show that densities derived from seismic velocities are around 2.68–2.83 g/cm^3 in the upper-middle crust and 2.88–2.96 g/cm^3 in the lower crust, whereas Welford and Hall (2013), using gravity inversion, obtained densities of 2.75–2.85 g/cm^3 for the upper-middle crust and 2.85–3.02 g/cm^3 for the lower crust. It should be stressed that the forward gravity modeling results presented in this study are non-unique and strongly biased by our seismic interpretation, the nature of the crustal domains, and the assigned densities.

4. Tectono-Stratigraphic Architecture of the Labrador Margin

The horizontal gradient of the Bouguer anomaly (Figure 2) highlights the existence of NW-SE and NNE to NE trending lineaments. The NW trending gravity lineaments found west of Chron 29 correlate well with the syn-rift normal faults interpreted along the seismic lines (Figure 3). They are associated with basement ridges corresponding to tilted blocks that formed during the stretching of the continental crust in the Cretaceous (Figure 3). The NNE to NE trending lineaments correlate with the fracture zones found in the Labrador Sea, namely from north to south, the Snorri Fracture Zone (SFZ), the Cartwright Fracture Zone

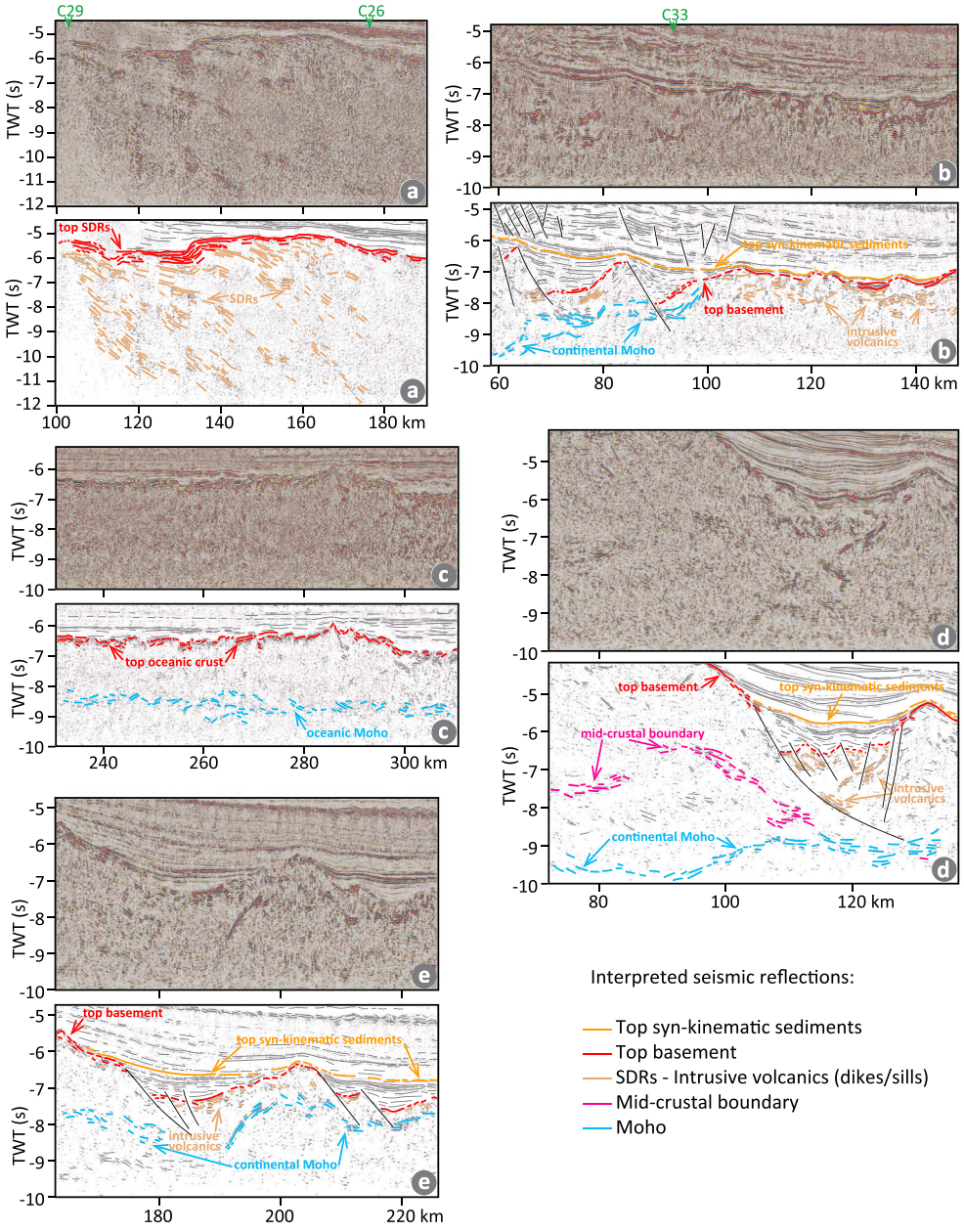

Figure 4. Close-up images of selected parts of the seismic data (see Figure 3).

(CFZ), the Minna Fracture Zone (MFZ), the Julinhaab Fracture Zone (JFZ), and the Charlie-Gibbs Fracture Zone (C-GFZ) (Srivastava & Roest, 1999).

The interpreted seismic lines (Figures 3 and 4) and the derived sediment isopach maps (Figure 5) depict the syn-tectonic and post-tectonic stratigraphic architectures of the Labrador margin. The Cretaceous syn-tectonic deposits (Figure 5a) are found in a NW trending basin parallel to the coastline and ending approximately at Chron 29. The syn-tectonic sedimentary depocenters south of the CFZ are located seaward of the continental slope and occupy a wide area, while north of the CFZ, they are located in a much narrower domain (Figure 5a). The thickness and distribution of the syn-tectonic package are controlled by the Cretaceous syn-rift extension, which is more pervasive seaward of the continental slope (Figures 4b, 4d, and 4e). Syn-rift structures in the continental shelf are limited to a few high-angle normal faults, mostly SW dipping, defining spatially isolated half grabens (Figures 3 and 4). In contrast, well-developed tilted continental blocks are observed in the deep basin of the margin, where major half grabens are bounded

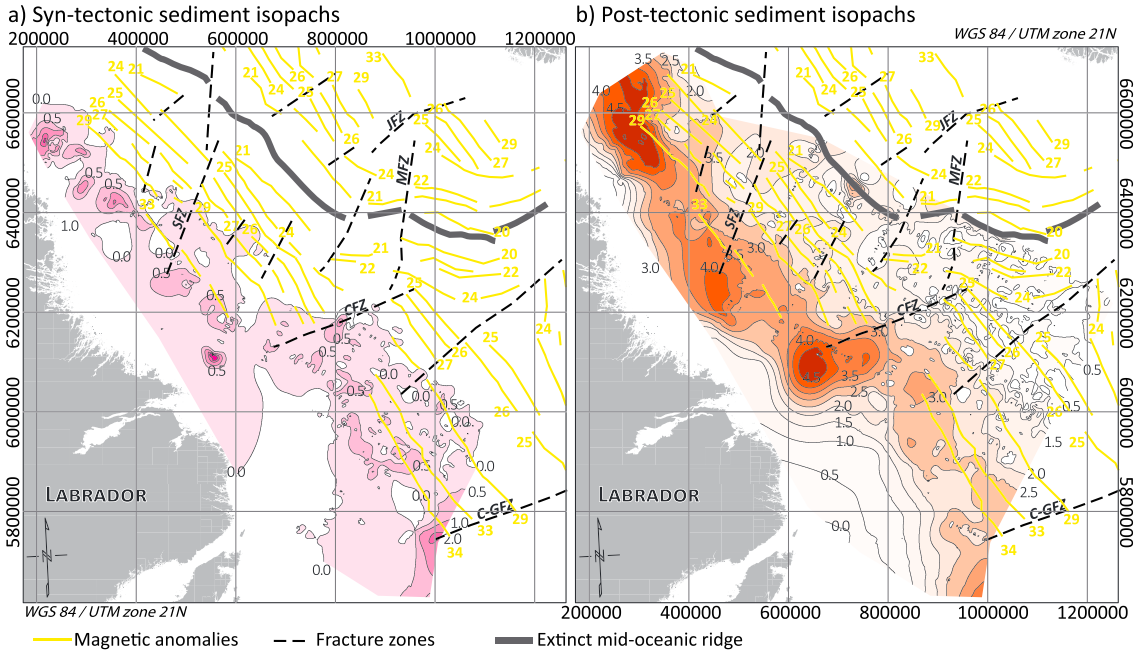

Figure 5. Maps of the Labrador margin showing the isopachs of the (a) syn-tectonic and (b) post-tectonic sedimentary packages. Thicknesses are two-way traveltime (TWT) in seconds.

by NE dipping normal faults and filled by relatively thick Cretaceous deposits (Figures 3, 4b, 4d, and 4e). The syn-rift geometry changes along strike and appears to be controlled by planar normal faults north of the CFZ (Figures 3b, 3c, and 4b) and by listric normal faults south of the CFZ (Figures 3d, 3e, 4d, and 4e). Overall, the listric geometry does not appear to be an artifact of the time domain and is preserved in most faults after depth conversion is carried out. On the other hand, the planar faults could become listric at greater depth, not imaged by the seismic lines (> 10 s twt). The planar faults in the north define narrower and deeper half-grabens (Figure 4b), while the listric faults in the south are associated with several antithetic and synthetic faults and define wider but shallower half-grabens (Figures 4d and 4e).

The post-tectonic package, composed of Cenozoic sediments, is thickest (up to 5 s twt) in the north (Figure 5b). The sediment isopach map shows several NW-SE elongated sedimentary depocenters located landward of Chron 26 in the north and landward of Chron 29 in the central and southern domains of the margin. These depocenters extend over the continental shelf, the continental slope, and the deep margin in the north, while in the south, they are mostly located seaward of the continental slope (Figure 5b).

5. Crustal Architecture of the Labrador Margin

The distinction between the different crust types along the seismic lines is based on the seismic character and the syn-rift structures observed in the acoustic basement. While, the continental crust is well defined underneath the continental shelf, characterized by relatively distinct semi-continuous reflections of high to moderate amplitudes, the seismic character of the COT is often ambiguous and changes along the margin, depending on the nature of the transition (i.e., magma poor vs magma rich). Thus, the landward boundary of the COT was assumed to roughly coincide with the oceanward limit of the main syn-rift structures (Figures 4b and 4e). The oceanic boundary is also unclear, especially in magma-poor setting where the initial oceanic spreading is usually characterized by reduced melt, leading to the formation of a proto-oceanic crust (Jagoutz et al., 2007). We define the oceanic boundary at the first frank oceanic crust (Figure 6), characterized in seismic by incoherent and discontinuous reflections of medium to low amplitudes (Figure 4c).

5.1. Continental and Oceanic Crust

The seaward termination of the continental crust appears to be consistent along the entire margin and coincides, approximately, with Chron 33. The first undisputable oceanic crust starts approximately at Chron 29

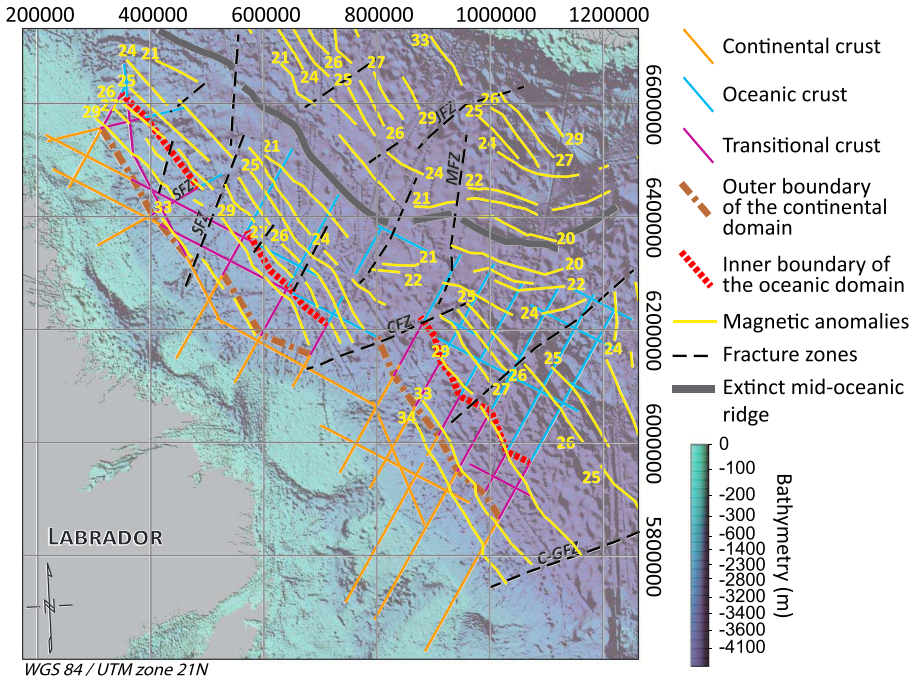

Figure 6. Map of the Labrador margin showing the continental and oceanic domains, identified along the seismic lines.

in the southern part of the margin (i.e., south of the CFZ), between Chrons 29 and 27 in the central part (i.e., between the CFZ and the SFZ), and around Chron 26 in the northern part (i.e., north of the SFZ) (Figure 6).

Several sets of discontinuous and high-amplitude reflections are imaged in the acoustic basement along the seismic lines (Figures 3 and 4). In the continental domain, the shallow high-amplitude reflections are interpreted to represent an intra-crustal level, which possibly marks the limit between the upper and lower crusts (Figure 4d). The deep high-amplitude reflections, which are more evident underneath the syn-rift tilted blocks in the distal margin, could represent the continental Moho (Figures 3d, 3e, 4b, 4d, and 4e). The high-amplitude reflections observed in the oceanic domain occur between −8 and −9 s (twt) and are interpreted to represent the oceanic Moho (Figures 3b, 3c, and 4c).

These high-amplitude reflections, representing intra-crustal discontinuities and possibly the Moho, are not observed along all seismic lines. Thus, to better constrain the crustal geometry in the entire margin, we use the free-air gravity anomalies (Sandwell et al., 2014) to model the thickness of the continental and oceanic crusts. Three gravity models are shown in Figure 7, illustrating the 2D crustal architecture in the northern (Figure 7a), central (Figure 7b), and southern (Figure 7c) segments of the margin. Figure 8 shows the interpolated isochores of the continental and oceanic crusts. The oceanic crust is 6- to 8-km thick in the southern and the central segments, and 8- to 10-km thick north of the SFZ. Thickness variations in the continental crust allow the distinction between three continental domains along the margin, namely, the weakly thinned proximal domain, the necking zone, and the highly extended distal domain (Figure 8). The proximal continental crust, partially covered by seismic data, mostly in the southern segment, is 22- to 28-km thick. The necking zone, characterized by a rapid thinning of the crust, is narrow in the south and widens toward the north. It is characterized by crustal thickness varying between 8 and 22 km in the northern and central segments, where it is located seaward of the continental slope. While north of the SFZ, the thickness of the crust in the necking zone varies between 26 and 2 km and underlies the continental shelf and slope (Figure 8). The distal continental crust is less than 8-km thick and 60- to 90-km wide south of the CFZ, narrows substantially north of the CFZ (25- to 35-km wide), and widens again near the SFZ (~ 70-km wide). In contrast, the northern segment (i.e., north of the SFZ) is characterized by a wide continental necking zone (~ 100 km) that ends with the complete thinning of the crust with practically no highly stretched continental domain (Figure 8).

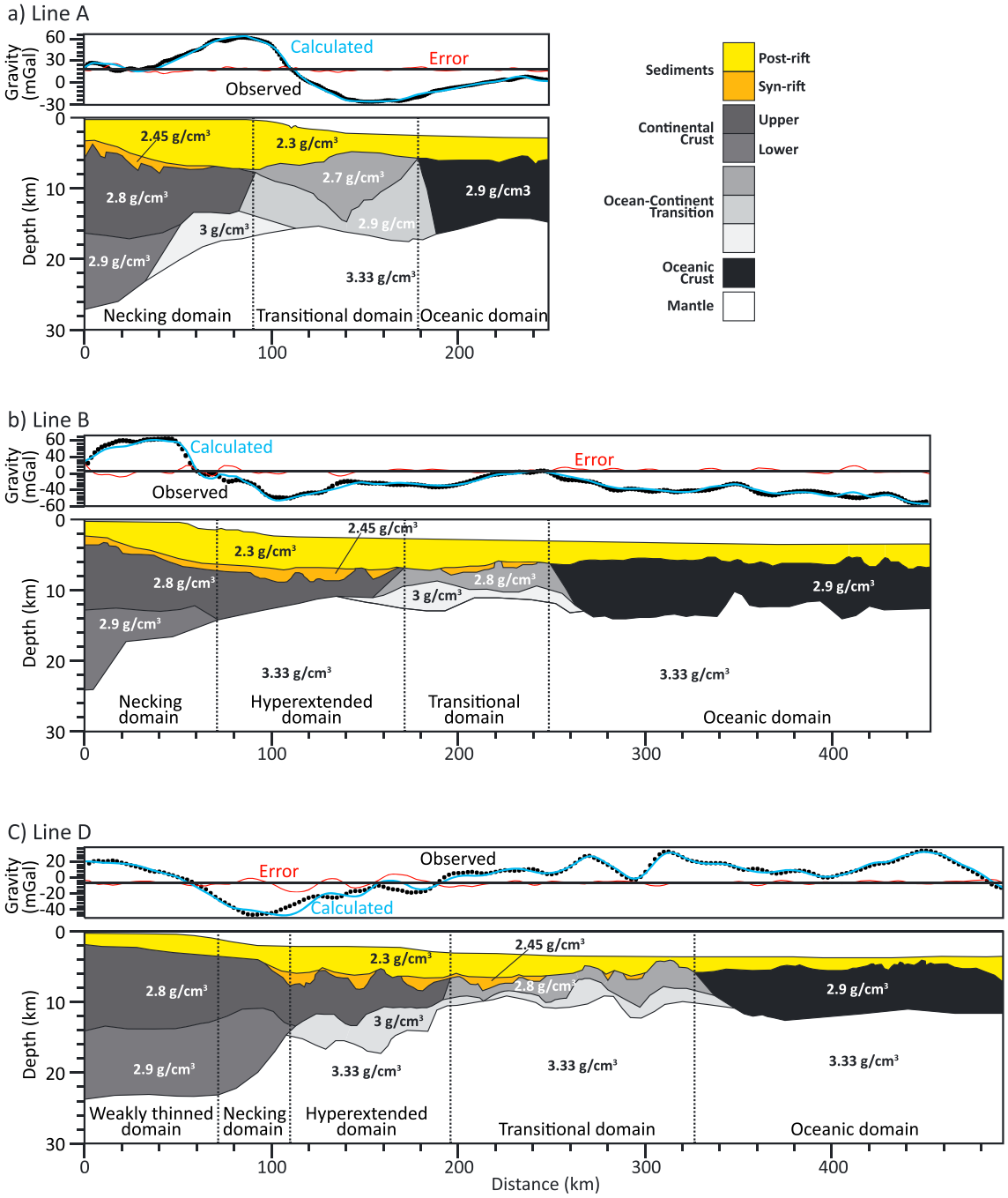

Figure 7. Gravity models showing the crustal structure along seismic lines A, B, and D. Models obtained using GM-SYS Profile Modelling (Geosoft) with public domain free-air gravity anomaly data (Sandwell et al., 2014).

5.2. Continent-Ocean Transition

The COT, defined by the outer termination of the continental crust and the first oceanic crust, consists of an 80- to 100-km wide domain, trending NW-SE and segmented by the CFZ and the SFZ (Figure 8). The character of seismic reflections in the COT, as imaged in the seismic lines, appears to change along the margin (Figure 3). In the northern segment, seismic line A shows two packages of high-amplitude reflections dipping oceanward in a wedge-like fashion (Figures 3a and 4a). In the central segment of the margin the COT is characterized by discontinuous and medium- to high-amplitude reflections (e.g., lines B and C;

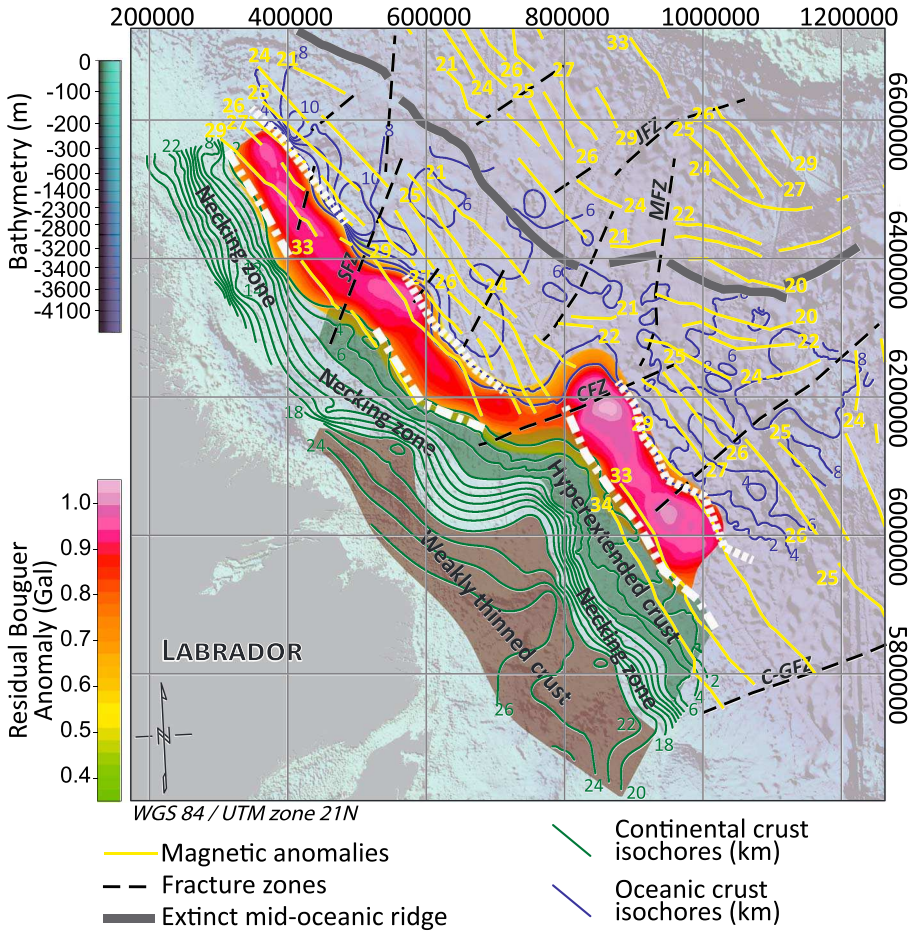

Figure 8. Map of the Labrador margin showing the thickness of the continental and ocean crusts, interpolated from the 2D gravity modeling along the seismic lines, and the residual gravity anomaly in the continent-ocean transition after removing the contribution of the Mesozoic sediment from the Bouguer anomaly.

Figures 3b, 3c, and 4b), whereas in the southern segment, it shows discontinuous and mostly transparent to low-amplitude reflections (e.g., lines D and E; Figures 3d and 3e).

Figure 8 shows the residual Bouguer anomaly in the COT domain after removing the contribution of the overlying Mesozoic sediments. It highlights variation along the COT domain, as illustrated by the seismic reflection character. Thus, high residual gravity anomaly is observed south of the CFZ (1.1–0.8 Gal), while low residual gravity anomaly occurs in the central segment between the SFZ and the CFZ (0.9–0.7 Gal). The northern segment shows intermediate residual gravity anomaly values (1.0–0.8 Gal). The depicted variations in the seismic reflection character and the gravity anomaly result from changes in the nature of the rocks forming the COT domain.

5.3. Previous Studies

Hosseinpour et al. (2013) and Welford and Hall (2013) examined crustal thicknesses in the entire Labrador Sea using gravity inversion. Their results are consistent with our forward gravity modeling as they show higher thinning of the continental crust south of the SFZ, with a COT domain that is wider in the south than in the north. Hosseinpour et al. (2013) proposed a plate reconstruction model for the Labrador Sea that suggests coeval initiation of rifting (~ 120 Ma) but diachronous transition from continental extension to initiation of COT crust formation (~ 85–69 Ma) and oceanic accretion (~ 69–63 Ma).

Recent studies by Keen et al. (2018a, 2018b) combined seismic and potential field data to characterize the structural and crustal architectures of the central and the northern parts of the Labrador margin. Their

work shows that the central segment of the Labrador margin is characterized by hyperextended continental crust and exhumed serpentinized mantle. While north of the SFZ, they show SDRs east of the continental necking zone. The proposed spatial distribution of the hyperextended crust and exhumed serpentinized mantle in the central Labrador margin and the SDRs in the northern Labrador margin is comparable with our interpretation (Figures 6 and 8).

Chalmers (1997) examined the nature of the crust along the conjugate SW Greenland margin using five seismic reflection lines and suggested an along-strike transition from a magma-rich margin in the north to a magma-poor margin in the south. He also interpreted a wider COT in the south with hyperextended crust and exhumed mantle, and a narrower COT in the north with SDRs and potential magmatic underplating under the necking zone.

6. Discussion

Seismic reflection and gravity data, presented above, illustrate the overall tectono-stratigraphic and crustal architectures of the Labrador margin. They reveal a segmented rifting evolution and a diachronous continental breakup.

6.1. Segmented Rifting

Three segments are identified along the margin, namely, the northern segment north of the SFZ, the southern segment south of the CFZ, and the central segment between the SFZ and the CFZ. The three segments of the margin show distinct crustal configurations with major differences in the geometry of the distal margin. The southern and central segments both consist of a narrow necking zone and a wide distal domain composed of a highly thinned continental crust and the COT. This is consistent with observations from the nearby magma-poor Newfoundland margin and indicates that the distal domain, in these two segments, formed by hyperextension, which led to the development of a very thin continental crust (< 10 km) and exhumed serpentinized subcontinental mantle in the COT (e.g., Péron-Pinvidic & Manatschal, 2009). The high-amplitude reflections, observed in the distal domain of the central segment (Figures 3b and 3c), indicate, however, the existence of volcanics, sills, and dikes. Seismic refraction data indicate that the COT in the central segment of the Labrador margin consists of a low-velocity upper layer (4–5 km/s) overlying a high-velocity (6.4–7.7 km/s) layer (Chian, Keen, et al., 1995). The proposed velocity interpretation suggests that the lower layer is serpentinized subcontinental mantle overlain by a basaltic layer (Chian, Keen, et al., 1995), which is consistent with our observations. The crustal geometry in the northern segment, on the other hand, is characterized by a wide necking zone and no hyperextended continental crust in the distal domain. Instead, SDRs are observed (Figure 3a), representing wedges of flood basalts in the COT, which is typical in magma-rich margins (e.g., Franke, 2013; Planke & Eldholm, 1994).

6.2. Diachronous Continental Breakup

In the southern and central segments of the margin, the inner boundary of the COT coincides with Chron 33 (ca. 80–79 Ma; Srivastava & Roest, 1999), indicating that the beginning of mantle exhumation was synchronous along most of the margin (Figure 6). In the north, the emplacement of SDRs started later around Chron 29 (ca. 65.8–64.4 Ma; Srivastava & Roest, 1999), which is concurrent with the passage of the proto-Iceland plume underneath the Davis Strait (Storey et al., 2007).

The outer boundary of the COT, indicating the first oceanic crust, varies from one segment to the other (Figure 6). It is concurrent to Chron 29 (ca. 65.8–64.4 Ma; Srivastava & Roest, 1999) in the south, between Chron 29 and Chron 27 (ca. 63.3–61.1 Ma; Srivastava & Roest, 1999) in the center, and around Chron 26 (ca. 60.5–57.7 Ma; Srivastava & Roest, 1999) in the north. This suggests a diachronous continental breakup with a younging of the onset of oceanic accretion toward the north of the margin.

Based on the distribution of magnetic Chrons in the COT, we can conclude that the transitional phase characterized by mantle exhumation in the south and emplacement of seaward dipping volcanic wedges in the north lasted around 15 Ma (between Chrons 33 and 29) and 8 Ma (between Chrons 29 and 26), respectively. While in magma-poor margins mantle exhumation can last several tens of millions of years before lithospheric breakup, in magma-rich margins the timing between the onset of magma formation and breakup is usually much shorter (< 5 Ma, Manatschal et al., 2015). In the case of the Iberian margin, where the

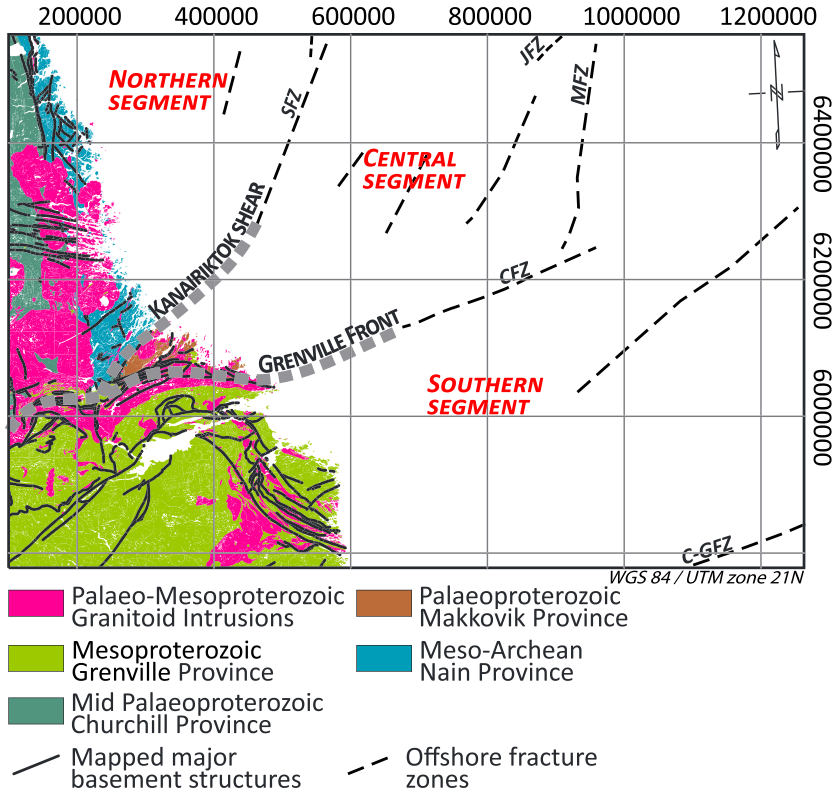

Figure 9. Simplified geological map of the onshore Labrador margin modified from Umpleby (1979), showing the different Precambrian domains and the major bounding structures. The onshore geological boundaries are correlated to the offshore fracture zones.

COT domain is much wider (up to 150 km wide) than in the Labrador margin (80- to 100-km wide), mantle exhumation lasted about 30 Myr (Manatschal et al., 2015).

6.3. Role of Inheritance in Rifting and Breakup

Previous studies have emphasized the role of the Labrador Sea fracture zones in accommodating variations in spreading direction and velocity during oceanic accretion (e.g., Srivastava & Roest, 1999). Our work indicates, however, that these fracture zones were also active and played a role in the late stage of rifting and continental breakup.

Prior to the Atlantic rifting, the CFZ and JFZ formed a continuous structure that extended east, south of Greenland, and west as part of the Grenville Front (Figures 1 and 9, Gower, 1996), which we label here as the Grenville Suture (GS). Similarly, the SFZ can be traced east into Greenland and west into the onshore Labrador as part of the Kanairiktok Shear Zone (Figures 1 and 9, Kerr et al., 1997), which we name here the Kanairiktok-Snorri Shear (KSS).

The final rifting stage in the Labrador margin is characterized by along-strike changes in the amount of hyperextension. The southern segment shows a wider hyperextended continental crust than the central segment. Although there is no evidence of stretched continental crust seaward of the necking zone in the northern segment, hyperextension could have taken place, then was overprinted by the volcanics. Nonetheless, it would have been much restricted given the narrow space between the necking zone and the oceanic domain. Alternatively, the breakup line may have switched across the SFZ, resulting in a hyperextended domain rather attached to the conjugate west Greenland margin. Such evolution, proposed for the central Atlantic for instance (Klingelhoefer et al., 2016), is in disagreement with observations from SW Greenland (Chalmers, 1997). The change in the amount of stretching along the Labrador margin was accommodated by left-lateral movements along the KSS and the GS prior to continental breakup.

The KSS and GS delimited three structural domains that were dismantled during the opening of the Labrador Sea: (1) the Archean North Atlantic Craton in the north, (2) the Paleoproterozoic Makkovik-Ketilidian Province in the center, and (3) the Mesoproterozoic Grenville Province in the south. The three structural domains form the continental basement of the northern, central, and southern segments, respectively, identified in the offshore Labrador Sea (Figure 9). Seismic refraction data from the Labrador continental shelf reveal that the crust is 35- to 40-km thick in the Makkovik domain but thickens to 50 km in the Grenville domain (Funck et al., 2001). Most importantly, this thickening is due to a 15- to 20-km thick high-velocity lower crustal wedge underlying the Grenville domain (Funck et al., 2001). This variability in crustal structure occurs at a more regional scale and is illustrated by the variations of surface heat flow recorded in the Canadian Shield. Data from the onshore Labrador margin show a noticeable southward increase in surface heat flow (Mareschal & Jaupart, 2004). Surface heat flow values range between 22 and 27 mW/m^2 in the Churchill and Nain Provinces, 27–37 mW/m^2 in the Makkovik Province, and 27–47 mW/m^2 in the Grenville Province. Mareschal and Jaupart (2004) argued that the spatial scale needs to be taken into account when explaining the origin of these variations in surface heat flow. Accordingly, local-scale variations, that is, within each province, are attributed to differences in crustal thickness resulting in changes in crustal radiogenic heat production, while regional-scale variations, that is, across provinces, are related to changes in lithospheric mantle heat flow. The increase in surface heat flow from the Makkovik to the Grenville is consistent with the observed crustal thickening south of the GS; however, the northward decrease in surface heat flow between the southern and northern Labrador is probably driven by a respective decrease in mantle heat flow. Although these are present-day heat flow values, the fact that they are consistent across each domain and toward the more stable shield interior implies that the observed variations persisted throughout their evolution.

The GS, in particular, was a major suture zone along which the Superior Province was subducted toward the SE underneath the Grenville Province, giving rise to calc-alkaline arcs (ca. 1.68 to 1.66 Ga; Gower, 1996). This magmatic event may have resulted in the depletion of the mantle underneath the Grenville domain, such as attested by the distribution of post-subduction magmatism that is found on both sides of the Labrador Sea but mostly north of the GS (Tappe et al., 2007). Furthermore, inversion of surface wave data depict lateral variations in shear velocity across the GS at depths ranging between 80 and 150 km, which suggests changes in both temperature and composition of the deep mantle lithosphere (Shapiro et al., 2004).

6.4. Influence of Lithospheric Strength on Stretching Nature

Lithospheric strength and extension rate are the main factors that dictate the mode of stretching during rifting (e.g., Huismans & Beaumont, 2003). The strength of the lithospheric layers is a function of their composition and the thermal structure. In general, a strong/cold upper lithosphere couples deformation effectively and produces a narrow and symmetric rift, while a weak/hot upper lithosphere decouples deformation between the brittle upper crust and upper mantle resulting in a wide and asymmetric rift (Buck, 1991; Huismans & Beaumont, 2003).

Observations from rifted margins indicate that during the early phase of rifting deformation is distributed over a wide domain, but as rifting evolves, deformation becomes localized (i.e., in the future distal margin) leading to the onset of crustal necking and ultimately continental breakup (e.g., Mohn et al., 2012). The transition from distributed to localized extension takes place once the crust is coupled to the mantle (Brune et al., 2014; Mohn et al., 2012; Péron-Pinvidic & Manatschal, 2009). The decoupling during early rifting is accommodated by the ductile part of the crust found below the brittle-ductile transition. The depth of the brittle-ductile transition and thus the thickness of the weak crustal layer are a function of crustal composition and geothermal gradient. In the case of a predominantly quartzo-feldspathic crust (i.e., felsic), the transition is expected at temperatures around 300 °C, while in a plagioclase-dominant crust (i.e., mafic) the transition occurs at about 500 °C (Ranalli, 2000; Stipp et al., 2002). Figure 10 shows theoretical strength profiles calculated for various lithospheric configurations, assuming different surface heat flows. Domains with a very low geothermal gradient (i.e., low surface heat flow) are characterized by a strong upper lithosphere where the crust and the mantle are strongly coupled at the initiation of stretching (Figure 10a). Domains with a higher surface heat flow tend to have a decoupled lithosphere (Figures 10b and 10c). In addition, the thickness of

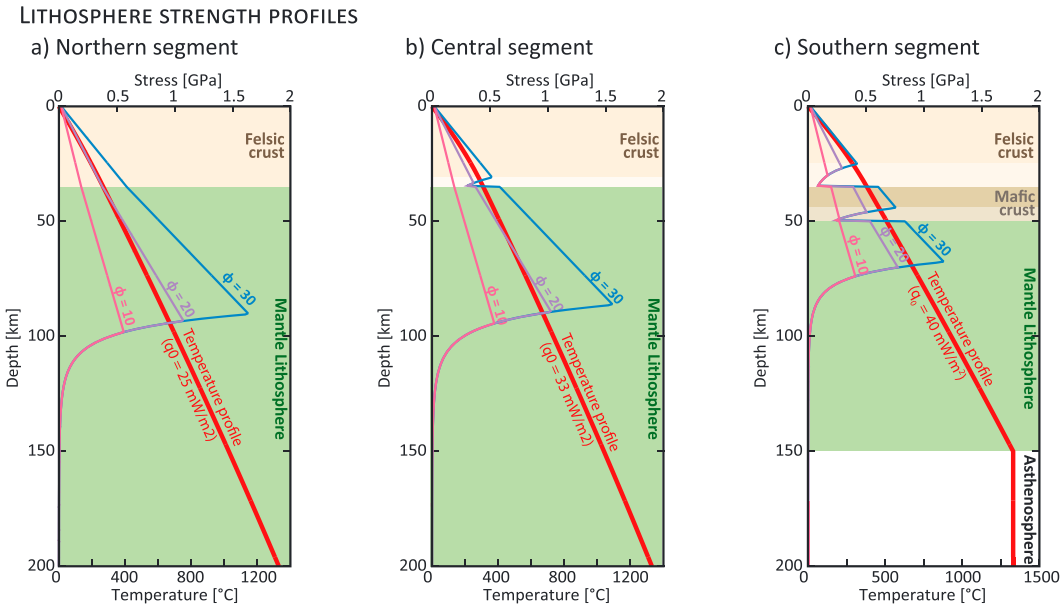

Figure 10. Theoretical pre-rift lithospheric strength profiles of the different segments of the Labrador margin calculated assuming power law creep parameters of wet quartz in the felsic crust (Gleason & Tullis, 1995), wet anorthite in the mafic crust (Rybacki & Dresen, 2000), wet olivine in the mantle (Karato & Wu, 1993), a strain rate of 10^{-15} s^{-1}, and different angles of internal friction (Φ). The geothermal gradients are calculated based on average surface heat flows (Q_0) derived from Mareschal and Jaupart (2004), assuming a uniform radiogenic heat production in the felsic crust, a thermal conductivity of 3 W/m/°C, and an isothermal mantle lithosphere at 1330 °C.

the decoupling ductile part of the crust increases with increasing thickness of the felsic crust (Figures 10b and 10c).

In the Labrador Sea, the inherited Precambrian structures (i.e., KSS and GS) delimit three domains with distinct pre-rift crustal architectures and varying thermal structures. The Archean domain, north of the KSS, is characterized by a very low surface heat flow (mean value of 25 mW/m^2) with a *normal* crustal thickness of 35 km and a 200-km thick cold lithosphere (Romanowicz & Yuan, 2010). The Paleoproterozoic domain, south of the KSS and north of the GS, is characterized by a slightly higher surface heat flow than the Archean domain (mean value of 33 mW/m^2) but a comparable lithospheric architecture with a 35-km thick crust and a 200-km thick lithosphere. The Mesoproterozoic domain, south of the GS, shows a higher surface heat flow (mean value of 40 mW/m^2) with a 50-km thick crust (35-km thick felsic upper crust and 15-km thick mafic lower crust; according to Funck et al., 2001) and a 150 km thick lithosphere (Shapiro et al., 2004). The calculated theoretical lithospheric strength profiles for the three domains based on the aforementioned boundary conditions show a strong and coupled pre-rift lithosphere in the northern Archean domain (Figure 10a), a relatively strong and decoupled pre-rift lithosphere in the central Paleoproterozoic domain (Figure 10b), and a weaker and decoupled pre-rift lithosphere in the southern Mesoproterozoic domain (Figure 10c). While in the central domain the decoupling ductile crust is only 5-km thick (assuming a friction angle of 30°), the southern domain is characterized by two decoupling layers at the base of the felsic upper crust and at the base of the mafic lower crust, which are approximately 10- and 6-km thick (Figure 10c), respectively.

The lateral change in the rheology of the pre-rift basement is responsible of the variations observed in the structural and crustal architectures along the Labrador margin, particularly, the southward increase in the thickness of the decoupling ductile crust, which can be correlated to an increase in ductile strain and a delay in the coupling of lithospheric deformation (Figure 11). Thus, at the time of coupling between the upper and lower crusts, the continental crust is thinner (i.e., more stretched) in the south than in the north. Since the crust needs to be thinned by a factor of 3 to 4 for mantle hydration to occur (Pérez-Gussinyé et al., 2001), hyperextension and mantle serpentinization and exhumation, which start after crustal coupling, were more enhanced in the southern segment of the margin (Figure 11). In the northern segment of the margin,

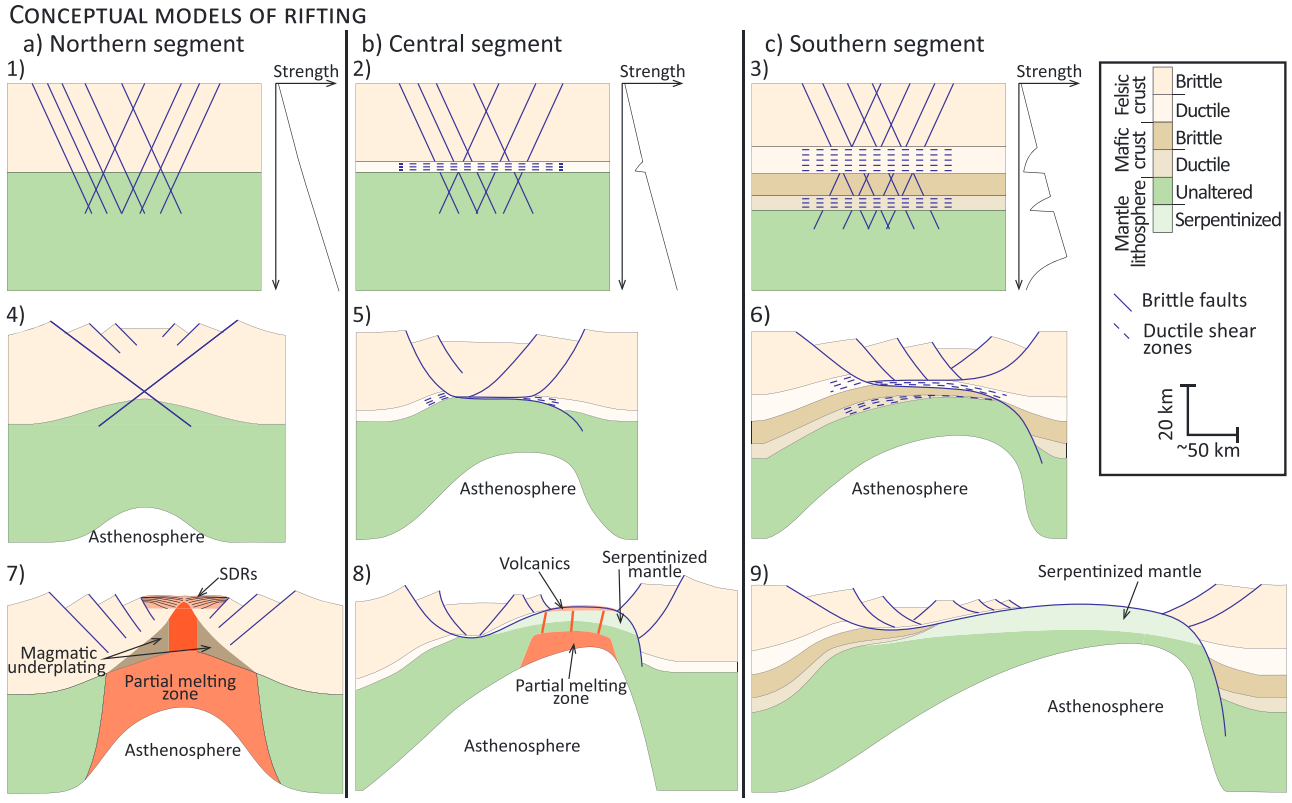

Figure 11. Conceptual models for the rift evolution of each segment of the Labrador Sea showing the initial lithospheric architecture: (1) strong and coupled lithosphere in the northern segment, (2) strong and decoupled lithosphere in the central segment, (3) weak and decoupled lithosphere in the southern segment. (4) In the northern segment deformation is mainly accommodated by pure shear extension. (5–6) In the central and southern segments deformation is initially accommodated by pure shear, but once the ductile crustal layers are thinned enough, the strong layers are coupled and simple shear extension takes over. (8–9) This leads to crustal hyperextension, mantle hydration (serpentinization), and exhumation before continental breakup, which occurs first in the southern segment (around Chron 29) and then in the central segment (between Chrons 29 and 27). The increase in mantle potential temperature due to the proto-Icelandic plume causes partial melting of the thinned Archean mantle lithosphere (i.e., north of the GS), which results in (7) SDR emplacement in the northern segment and magma-rich continental breakup (around Chron 26). Partial melting occurs also underneath the central segment but to a lesser extent due to the prior mantle hydration. It resulted in volcanics intruding and overlying the serpentinized exhumed mantle (8).

the lack of apparent syn-rift structures in the necking zone prevent us from understanding the style of rifting before the emplacement of SDRs. Numerical modeling shows that stretching of a strong and coupled crust starts as pure shear but can evolve into simple shear only if the lower crust is weakened and can accommodate some ductile strain (Huismans & Beaumont, 2003). In any case, the amount of crustal stretching in the north was much less than in the south and given the pre-rift cold thermal structure of the lithosphere, SDR emplacement and continental breakup were only possible due to the thermal anomaly provided by the passage of the proto-Icelandic plume. In addition, the inherited mantle composition favored an Early Paleocene volcanism restricted to the northern segment of the margin, north of the GS, characterized by a more *fertile* Archean mantle.

7. Conclusions

The initial rheology of the lithosphere controls the style of extension during rifting and has a major influence on the final crustal architecture of rifted margins. In the case of a hot geothermal gradient (i.e., high surface heat flow), the lithosphere is weak and deformation is decoupled at first. The decoupling is controlled by the weak parts of the crust found below the brittle-ductile transition. An increase in the thickness of the ductile crust increases the amount of ductile strain accommodated by the lithosphere, which delays the coupling of the brittle crust and the brittle mantle lithosphere. This enhances mantle hydration, continental hyperextension, and mantle exhumation in the COT. In the case of a cold geothermal gradient (i.e., low surface heat flow), the lithosphere is strong and deformation is most likely to be coupled between the crust and the

upper mantle lithosphere. Deformation is accommodated mostly by pure shear with no (or very limited) hyperextension and mantle exhumation.

Variation in the amount of volcanics in the COT domain is controlled not only by the geometry of rifting but also by the fertility of the base of the mantle lithosphere and the timing and the degree of mantle melting, in relation to lithospheric thinning and mantle hydration.

Thus, inherited heterogeneities in the composition and thickness of the lithospheric layers and their thermal structure affect rifting geometry, crustal architecture, and magmatic budget during breakup along rifted margins.

Acknowledgments
Seismic data used in this work were provided by TGS for research purposes. High-resolution images of seismic lines A, B, C, D, and E are attached as supporting information. We would like to thank the Editor Claudio Faccenna, Per Terje Osmundsen, and the other three anonymous reviewers for their comments and feedback, which helped improve the initial version of the manuscript.

References

Alves, T. M., Moita, C., Cunha, T., Ullnaess, M., Myklebust, R., Monteiro, J. H., & Manuppella, G. (2009). Diachronous evolution of Late Jurassic–Cretaceous continental rifting in the northeast Atlantic (west Iberian margin). *Tectonics*, *28*, TC4003. https://doi.org/10.1029/2008TC002337

Balkwill, H. R., & McMillan, N. J. (1990). Mesozoic–Cenozoic geology of the Labrador shelf. In M. J. Keen & G. L. Williams (Eds.), *Geology of the continental margin of eastern Canada, geology of Canada* (Vol. 2, pp. 31–85).

Brune, S., Heine, C., Pérez-Gussinyé, M., & Sobolev, S. V. (2014). Rift migration explains continental margin asymmetry and crustal hyper-extension. *Nature Communications*, *5*. https://doi.org/10.1038/ncomms5014

Buck, W. R. (1991). Modes of continental lithospheric extension. *Journal of Geophysical Research*, *96*(B12), 20,161–20,178. https://doi.org/10.1029/91JB01485

Chalmers, J. A. (1997). The continental margin off southern Greenland: Along-strike transition from an amagmatic to a volcanic margin. *Journal of the Geological Society*, *154*(3), 571–576. https://doi.org/10.1144/gsjgs.154.3.0571

Chalmers, J. A., & Laursen, K. H. (1995). Labrador Sea: The extent of continental and oceanic crust and the timing of the onset of seafloor spreading. *Marine and Petroleum Geology*, *12*(2), 205–217. https://doi.org/10.1016/0264-8172(95)92840-S

Chian, D., Keen, C. E., Reid, I., & Louden, K. E. (1995). Evolution of nonvolcanic rifted margins: New results from the conjugate margins of the Labrador Sea. *Geology*, *23*(7), 589–592. https://doi.org/10.1130/0091-7613(1995)023<0589:EONRMN>2.3.CO;2

Chian, D., Louden, K. E., & Reid, I. (1995). Crustal structure of the Labrador Sea conjugate margin and implications for the formation of nonvolcanic continental margins. *Journal of Geophysical Research*, *100*(B12), 24,239–24,253. https://doi.org/10.1029/95JB02162

Culshaw, N., Brown, T., Reynolds, P. H., & Ketchum, J. W. (2000). Kanairiktok shear zone: The boundary between the Paleoproterozoic Makkovik Province and the Archean Nain Province, Labrador, Canada. *Canadian Journal of Earth Sciences*, *37*(9), 1245–1257. https://doi.org/10.1139/e00-035

Dickie, K., Keen, C. E., Williams, G. L., & Dehler, S. A. (2011). Tectonostratigraphic evolution of the Labrador margin, Atlantic Canada. *Marine and Petroleum Geology*, *28*(9), 1663–1675. https://doi.org/10.1016/j.marpetgeo.2011.05.009

Epin, M.-E., & Manatschal, G. (2018). Three-dimensional architecture, structural evolution, and role of inheritance controlling detachment faulting at a hyperextended distal margin: The example of the err detachment system (SE Switzerland). *Tectonics*, *37*, 4494–4514. https://doi.org/10.1029/2018TC005125

Franke, D. (2013). Rifting, lithosphere breakup and volcanism: Comparison of magma-poor and volcanic rifted margins. *Marine and Petroleum Geology*, *43*, 63–87. https://doi.org/10.1016/j.marpetgeo.2012.11.003

Funck, T., Hansen, A. K., Reid, I. D., & Louden, K. E. (2008). The crustal structure of the southern Nain and Makkovik Provinces of Labrador derived from refraction seismic data. *Canadian Journal of Earth Sciences*, *45*(4), 465–481. https://doi.org/10.1139/E08-007

Funck, T., Jackson, H. R., Louden, K. E., & Klingelhöfer, F. (2007). Seismic study of the transform-rifted margin in Davis Strait between Baffin Island (Canada) and Greenland: What happens when a plume meets a transform. *Journal of Geophysical Research*, *112*, B04402. https://doi.org/10.1029/2006JB004308

Funck, T., Louden, K. E., & Reid, I. D. (2001). Crustal structure of the Grenville Province in southeastern Labrador from refraction seismic data: Evidence for a high-velocity lower crustal wedge. *Canadian Journal of Earth Sciences*, *38*(10), 1463–1478. https://doi.org/10.1139/e01-026

Geoffroy, L., Burov, E. B., & Werner, P. (2015). Volcanic passive margins: Another way to break up continents. *Scientific Reports*, *5*, 14,828. https://doi.org/10.1038/srep14828

Gleason, G. C., & Tullis, J. (1995). A flow law for dislocation creep of quartz aggregates determined with the molten salt cell. *Tectonophysics*, *247*(1-4), 1–23. https://doi.org/10.1016/0040-1951(95)00011-B

Gouiza, M., Hall, J., & Welford, J. K. (2017). Tectono-stratigraphic evolution and crustal architecture of the Orphan Basin during North Atlantic rifting. *International Journal of Earth Sciences*, *106*(3), 917–937. https://doi.org/10.1007/s00531-016-1341-0

Gower, C. F. (1996). The evolution of the Grenville Province in eastern Labrador, Canada. *Geological Society, London, Special Publications*, *112*(1), 197–218. https://doi.org/10.1144/GSL.SP.1996.112.01.11

Hosseinpour, M., Müller, R. D., Williams, S. E., & Whittaker, J. M. (2013). Full-fit reconstruction of the Labrador Sea and Baffin Bay. *Solid Earth*, *4*(2), 461–479. https://doi.org/10.5194/se-4-461-2013

Huismans, R. S., & Beaumont, C. (2003). Symmetric and asymmetric lithospheric extension: Relative effects of frictional-plastic and viscous strain softening. *Journal of Geophysical Research*, *108*(B10), 2496. https://doi.org/10.1029/2002JB002026

Jagoutz, O., Müntener, O., Manatschal, G., Rubatto, D., Péron-Pinvidic, G., Turrin, B. D., & Villa, I. M. (2007). The rift-to-drift transition in the North Atlantic: A stuttering start of the MORB machine? *Geology*, *35*(12), 1087–1090. https://doi.org/10.1130/G23613A.1

Karato, S., & Wu, P. (1993). Rheology of the upper mantle: A synthesis. *Science*, *260*(5109), 771–778. https://doi.org/10.1126/science.260.5109.771

Keen, C. E., Dickie, K., & Dehler, S. A. (2012). The volcanic margins of the northern Labrador Sea: Insights to the rifting process: VOLCANIC MARGINS, NORTHERN LABRADOR SEA. *Tectonics*, *31*, TC1011. https://doi.org/10.1029/2011TC002985

Keen, C. E., Dickie, K., & Dafoe, L. T. (2018a). Structural characteristics of the ocean-continent transition along the rifted continental margin, offshore central Labrador. *Marine and Petroleum Geology*, *89*, 443–463. https://doi.org/10.1016/j.marpetgeo.2017.10.012

Keen, C. E., Dickie, K., & Dafoe, L. T. (2018b). Structural evolution of the rifted margin off northern Labrador: The role of hyperextension and magmatism. *Tectonics*, *37*(7), 1955–1972. https://doi.org/10.1029/2017TC004924

Kerr, A., Hall, J., Wardle, R. J., Gower, C. F., & Ryan, B. (1997). New reflections on the structure and evolution of the Makkovikian - Ketilidian orogen in Labrador and southern Greenland. *Tectonics*, *16*(6), 942–965. https://doi.org/10.1029/97TC02286

Klingelhoefer, F., Biari, Y., Sahabi, M., Aslanian, D., Schnabel, M., Matias, L., et al. (2016). Crustal structure variations along the NW-African continental margin: A comparison of new and existing models from wide-angle and reflection seismic data. *Tectonophysics*, *674*, 227–252. https://doi.org/10.1016/j.tecto.2016.02.024

Larsen, L. M., Heaman, L. M., Creaser, R. A., Duncan, R. A., Frei, R., & Hutchison, M. (2009). Tectonomagmatic events during stretching and basin formation in the Labrador Sea and the Davis Strait: Evidence from age and composition of Mesozoic to Palaeogene dyke swarms in west Greenland. *Journal of the Geological Society*, *166*(6), 999–1012. https://doi.org/10.1144/0016-76492009-038

Lavecchia, A., Thieulot, C., Beekman, F., Cloetingh, S., & Clark, S. (2017). Lithosphere erosion and continental breakup: Interaction of extension, plume upwelling and melting. *Earth and Planetary Science Letters*, *467*, 89–98. https://doi.org/10.1016/j.epsl.2017.03.028

Manatschal, G. (2004). New models for evolution of magma-poor rifted margins based on a review of data and concepts from West Iberia and the Alps. *International Journal of Earth Sciences*, *93*(3). https://doi.org/10.1007/s00531-004-0394-7

Manatschal, G., Lavier, L., & Chenin, P. (2015). The role of inheritance in structuring hyperextended rift systems: Some considerations based on observations and numerical modeling. *Gondwana Research*, *27*(1), 140–164. https://doi.org/10.1016/j.gr.2014.08.006

Mareschal, J. C., & Jaupart, C. (2004). Variations of surface heat flow and lithospheric thermal structure beneath the north American craton. *Earth and Planetary Science Letters*, *223*(1–2), 65–77. https://doi.org/10.1016/j.epsl.2004.04.002

Mohn, G., Manatschal, G., Beltrando, M., Masini, E., & Kusznir, N. (2012). Necking of continental crust in magma-poor rifted margins: Evidence from the fossil Alpine Tethys margins. *Tectonics*, *31*, TC1012. https://doi.org/10.1029/2011TC002961

Nutman, A. P., Friend, C. R. L., Barker, S. L. L., & McGregor, V. R. (2004). Inventory and assessment of Palaeoarchaean gneiss terrains and detrital zircons in southern West Greenland. *Precambrian Research*, *135*(4), 281–314. https://doi.org/10.1016/j.precamres.2004.09.002

Osmundsen, P. T., & Ebbing, J. (2008). Styles of extension offshore mid-Norway and implications for mechanisms of crustal thinning at passive margins. *Tectonics*, *27*, TC6016. https://doi.org/10.1029/2007TC002242

Osmundsen, P. T., Péron-Pinvidic, G., Ebbing, J., Erratt, D., Fjellanger, E., Bergslien, D., & Syvertsen, S. E. (2016). Extension, hyperextension and mantle exhumation offshore Norway: A discussion based on 6 crustal transects. *Norwegian Journal of Geology*, *96*(4), 343–372. https://doi.org/10.17850/njg96-4-05

Paton, D. A., Pindell, J., McDermott, K., Bellingham, P., & Horn, B. (2017). Evolution of seaward-dipping reflectors at the onset of oceanic crust formation at volcanic passive margins: Insights from the South Atlantic. *Geology*, *45*(5), 439–442. https://doi.org/10.1130/G38706.1

Peace, A., McCaffrey, K., Imber, J., Phethean, J., Nowell, G., Gerdes, K., & Dempsey, E. (2016). An evaluation of Mesozoic rift-related magmatism on the margins of the Labrador Sea: Implications for rifting and passive margin asymmetry. *Geosphere*, *12*(6), 1701–1724. https://doi.org/10.1130/GES01341.1

Pérez-Gussinyé, M., Reston, T. J., & Morgan, J. P. (2001). Serpentinization and magmatism during extension at non-volcanic margins: The effect of initial lithospheric structure. *Geological Society, London, Special Publications*, *187*(1), 551–576. https://doi.org/10.1144/GSL.SP.2001.187.01.27

Péron-Pinvidic, G., & Manatschal, G. (2009). The final rifting evolution at deep magma-poor passive margins from Iberia-Newfoundland: A new point of view. *International Journal of Earth Sciences*, *98*(7), 1581–1597. https://doi.org/10.1007/s00531-008-0337-9

Péron-Pinvidic, G., Osmundsen, P. T., & Ebbing, J. (2016). Mismatch of geophysical datasets in distal rifted margin studies. *Terra Nova*, *28*(5), 340–347. https://doi.org/10.1111/ter.12226

Planke, S., & Eldholm, O. (1994). Seismic response and construction of seaward dipping wedges of flood basalts: Vøring volcanic margin. *Journal of Geophysical Research*, *99*(B5), 9263–9278. https://doi.org/10.1029/94JB00468

Pouliquen, G., Connard, G., Kearns, H., Gouiza, M., & Paton, D. (2017). Public domain satellite gravity inversion offshore Somalia combining layered-Earth and voxel based modelling. *First Break*, *35*(9), 73–79.

Ranalli, G. (2000). Rheology of the crust and its role in tectonic reactivation. *Journal of Geodynamics*, *30*(1-2), 3–15. https://doi.org/10.1016/S0264-3707(99)00024-1

Romanowicz, B., & Yuan, H. (2010). Lithospheric layering in the North American craton. *Nature*, *466*(7310), 1063. https://doi.org/10.1038/nature09332

Rybacki, E., & Dresen, G. (2000). Dislocation and diffusion creep of synthetic anorthite aggregates. *Journal of Geophysical Research*, *105*(B11), 26,017–26,036. https://doi.org/10.1029/2000JB900223

Sandwell, D. T., Müller, R. D., Smith, W. H. F., Garcia, E., & Francis, R. (2014). New global marine gravity model from CryoSat-2 and Jason-1 reveals buried tectonic structure. *Science*, *346*(6205), 65–67. https://doi.org/10.1126/science.1258213

Shapiro, N. M., Ritzwoller, M. H., Mareschal, J. C., & Jaupart, C. (2004). Lithospheric structure of the Canadian Shield inferred from inversion of surface-wave dispersion with thermodynamic a priori constraints. *Geological Society, London, Special Publications*, *239*(1), 175–194. https://doi.org/10.1144/GSL.SP.2004.239.01.12

Soares, D. M., Alves, T. M., & Terrinha, P. (2012). The breakup sequence and associated lithospheric breakup surface: Their significance in the context of rifted continental margins (West Iberia and Newfoundland margins, North Atlantic). *Earth and Planetary Science Letters*, *355*, 311–326. https://doi.org/10.1016/j.epsl.2012.08.036

Srivastava, S. P., & Roest, W. R. (1999). Extent of oceanic crust in the Labrador Sea. *Marine and Petroleum Geology*, *16*(1), 65–84. https://doi.org/10.1016/S0264-8172(98)00041-5

Stipp, M., Stünitz, H., Heilbronner, R., & Schmid, S. M. (2002). Dynamic recrystallization of quartz: Correlation between natural and experimental conditions. *Geological Society, London, Special Publications*, *200*(1), 171–190. https://doi.org/10.1144/GSL.SP.2001.200.01.11

Storey, M., Duncan, R. A., & Tegner, C. (2007). Timing and duration of volcanism in the North Atlantic Igneous Province: Implications for geodynamics and links to the Iceland hotspot. *Chemical Geology*, *241*(3-4), 264–281. https://doi.org/10.1016/j.chemgeo.2007.01.016

Suckro, S. K., Gohl, K., Funck, T., Heyde, I., Ehrhardt, A., Schreckenberger, B., et al. (2012). The crustal structure of southern Baffin Bay: Implications from a seismic refraction experiment. *Geophysical Journal International*, *190*(1), 37–58. https://doi.org/10.1111/j.1365-246X.2012.05477.x

Sutra, E., & Manatschal, G. (2012). How does the continental crust thin in a hyperextended rifted margin? Insights from the Iberia margin. *Geology*, *40*(2), 139–142. https://doi.org/10.1130/G32786.1

Tappe, S., Foley, S. F., Stracke, A., Romer, R. L., Kjarsgaard, B. A., Heaman, L. M., & Joyce, N. (2007). Craton reactivation on the Labrador Sea margins: 40Ar/39Ar age and Sr–Nd–Hf–Pb isotope constraints from alkaline and carbonatite intrusives. *Earth and Planetary Science Letters*, *256*(3-4), 433–454. https://doi.org/10.1016/j.epsl.2007.01.036

Tucholke, B. E., Sawyer, D. S., & Sibuet, J.-C. (2007). Breakup of the Newfoundland–Iberia rift. *Geological Society, London, Special Publications*, *282*(1), 9–46. https://doi.org/10.1144/SP282.2

Umpleby, D. (1979). Geology of the Labrador shelf. Geological Survey of Canada.

Van Kranendonk, M. J., St-Onge, M. R., & Henderson, J. R. (1993). Paleoproterozoic tectonic assembly of northeast Laurentia through multiple indentations. *Precambrian Research*, *63*(3-4), 325–347. https://doi.org/10.1016/0301-9268(93)90039-5

Wardle, R. J., Paltanavage, A., Nolan, L., & Leawood, T. (1997). Geological map of Labrador. Geoscience Publications and Information Section, Geological Survey, Department of Mines and Energy, Government of Newfoundland and Labrador.

Welford, J. K., & Hall, J. (2013). Lithospheric structure of the Labrador Sea from constrained 3-D gravity inversion. *Geophysical Journal International*, *195*(2), 767–784. https://doi.org/10.1093/gji/ggt296

Wittig, N., Webb, M., Pearson, D. G., Dale, C. W., Ottley, C. J., Hutchison, M., et al. (2010). Formation of the North Atlantic craton: Timing and mechanisms constrained from Re–Os isotope and PGE data of peridotite xenoliths from S.W. Greenland. *Chemical Geology*, *276*(3–4), 166–187. https://doi.org/10.1016/j.chemgeo.2010.06.002